[Article] doi: 10.3866/PKU.WHXB201512241 www.whxb.pku.edu.cn

四丁基季鏻羧酸盐离子液体的物理化学性质与CO_2溶解度

陈凤凤 董 艳 桑晓燕 周 言* 陶端健*
(江西师范大学化学化工学院，南昌 330022)

摘要：在298.15−348.15 K温度范围内，测定了四种四丁基季鏻羧酸盐离子液体([P_{4444}][CA])的密度、粘度、折射率、电导率等物理化学性质，得出了其随温度的变化关系，并获得了不同温度下该类离子液体的热膨胀系数。其次，在1个大气压和313.15 K温度下，测定了CO_2在该类离子液体中的溶解度，结果表明，四丁基季鏻丁酸盐吸收CO_2的性能最好，吸收量为0.4 mol·mol^{-1}，平衡时间小于5 min。

关键词：离子液体；四丁基季鏻羧酸盐；物理化学性质；CO_2吸收
中图分类号：O642

Physicochemical Properties and CO_2 Solubility of Tetrabutylphosphonium Carboxylate Ionic Liquids

CHEN Feng-Feng DONG Yan SANG Xiao-Yan ZHOU Yan* TAO Duan-Jian*
(*College of Chemistry and Chemical Engineering*, *Jiangxi Normal University, Nanchang 330022*, *P. R. China*)

Abstract: Four tetrabutylphosphonium carboxylate ionic liquids ([P_{4444}][CA]) were prepared, and their densities, viscosities, refractive indices, and conductivities were measured and correlated with thermodynamic and empirical equations in the temperature range of 298.15−348.15 K. The influence of temperature on these four properties of [P_{4444}][CA] was discussed, and their thermal expansion coefficient values were calculated. The CO_2 absorption capacity of [P_{4444}][CA] was studied at 313.15 K and 100 kPa. The results indicated that [P_{4444}][Buty] had the highest CO_2 capture capacity among these ionic liquids, with an absorption capacity of 0.4 mol·mol^{-1} and balance time of less than 5 min.

Key Words: Ionic liquid; Tetrabutylphosphonium carboxylate; Physicochemical property; CO_2 capture

1 Introduction

In recent years, ionic liquids (ILs) have attracted increasing attention as promising catalysts and green solvents. Most ILs possess many specific properties such as structural designability, low volatility, high thermal and chemical stability, and outstanding solubility[1−3]. Thus, these features can afford a lot of opportunities for the applications of ILs in many fields such as gas absorption, organic synthesis, catalysis, electrochemistry, biotransformation, etc[3−7].

Recently, carboxylate ionic liquids (CAILs), as being a prototype of basic ILs, have been widely reported for Michael addition, Knoevenagel condensation, dissolution of cellulose and other reactions[8−14]. For example, Liang *et al*.[12] reported that the catalysis of 1,1,3,3-tetramethylguanidine acetate ([TMG][Ace]) was applied in the alcoholysis of propylene oxide. Cao *et al*.[13] reported that 1-ethyl-3-methylimidazolium acetate showed a much higher ability to dissolve cellulose. We also used tetrabutylphosphonium carboxylate ILs as catalysts for highly efficient

Received: September 11, 2015; Revised: December 23, 2015; Published on Web: December 24, 2015.
*Corresponding authors. TAO Duan-Jian, Email: djtao@jxnu.edu.cn. ZHOU Yan, Email: anitachow@jxnu.edu.cn; Tel: +86-791-88120317.
The project was supported by the National Natural Science Foundations of China (21206063, 21566011, 31570560), Natural Science Foundations of Jiangxi Provincial Department of Science and Technology, China (20151BAB213016), and Sponsored Program for Cultivating Youths of Outstanding Ability in Jiangxi Normal University, China.
国家自然科学基金(21206063, 21566011, 31570560), 江西省自然科学基金(20151BAB213016)及江西师范大学青年英才计划项目资助

synthesis of propylene glycol methyl ether[14]. However, in order to develop industrial applications of CAILs, there is an urgent need to study the fundamental physicochemical properties of CAILs including density, viscosity, refractive index, conductivity, etc.

Till now, a few physicochemical property investigations have been made involving cholinium carboxylate ILs[15], tetraalkylammonium carboxylate ILs[16], imidazolium carboxylate ILs[17−23]. The physicochemical properties of phosphonium carboxylate ILs have not been studied systematically yet. As our continuous work on the utilization of phosphonium carboxylate ILs in sustainable catalysis, it is very worth noting that to date the properties of such phosphonium carboxylate ILs remain unknown.

In this work, four CAILs, tetrabutylphosphonium formate ([P_{4444}][For]), tetrabutylphosphonium acetate ([P_{4444}][Ace]), tetrabutylphosphonium propionate ([P_{4444}][Prop]), tetrabutylphosphonium butyrate ([P_{4444}][Buty]) were prepared, and their physicochemical properties (density, viscosity, refractive index, and conductivity) were measured and correlated with thermodynamic and empirical equations. The CO_2 solubility of these CAILs was also studied at 313.15 K and atmosphere pressure.

2 Experimental

2.1 Materials

Tetrabutylphosphonium bromide (mass purity ≥ 98%) and anion exchange resin Amberlite 717 were purchased from Aladdin Chemical Reagent Co. Ltd. (Shanghai, China). CO_2 with a mass purity of 99.999% was purchased from Jiangxi Province Specialty Gases. Formic acid, acetic acid, propionic acid, butyric acid, and ethanol were of analytical grade and used without any further purification, which were purchased from Tianjin Fuchen Chemical Reagent Co. Ltd. (China). Doubly distilled water was used in all experiments.

The synthesis and characterization of [P_{4444}][CA] ILs had been described in our previous work (Scheme 1)[14]. The water content was less than 0.1% (*w*, mass fraction) in each [P_{4444}][CA] IL, which was analyzed by Karl Fischer titration (Metrohm 756 KF coulometer). The concentration of Br^- in each [P_{4444}][CA] IL was measured by Mohr titration, and the related impurity was less than 0.02% (*w*).

2.2 Physicochemical properties

All of [P_{4444}][CA] ILs were dried in vacuum at 353.15 K before measuring the properties. Densities were measured over the temperature range of 293.15 − 353.15 K by an Anton Paar densimeter (model DMA4500), which was checked by dry air and doubly distilled water. The precision of the density values was $\pm10^{-5}$ g·cm^{-3} with a temperature accuracy of ±0.05 K. Viscosities were measured by a cone-plate viscometer (Brookfield DV II+ Pro) with a temperature control of ±0.05 K, and the precision of the viscosity values was $\pm10^{-2}$ mPa·s. The instrument was calibrated using standard calibration fluids such as ethanol and glycol with known viscosities. The temperature range was from 298.15 to 348.15 K, and the attaining thermal equilibrium time was about 30 min. Refractive indices were recorded with a Rudolph research analytical J357 refractometer at temperatures from 298.15 to 348.15 K. The precision of refractive indices values was $\pm10^{-4}$ with a temperature accuracy of ±0.05 K. Apparatus was calibrated and checked by pure organic solvents with known refractive index before each series of measurements[24]. Conductivity was determined in the temperature range from 298.15 to 348.15 K (Conductivity meter DDJS-308A, Shanghai Leici Company) with a DJS-1C electrode. Caution was taken to prevent evaporation, and the electrode and the solution were sealed in typical glassware, which was immersed into a thermostatic bath with a temperature accuracy of ±0.05 K. The precision of the conductivity values was ±0.1 μS·cm^{-1}.

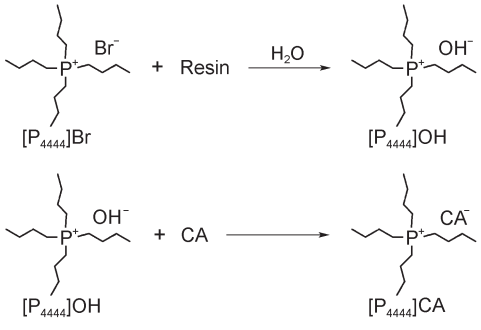

Scheme 1 General route for the synthesis of [P_{4444}][CA] ILs

2.3 Determination of CO_2 absorption

The apparatus for the determination of CO_2 absorption in [P_{4444}][CA] ILs is similar to that in the previous reference (Fig.1)[25]. The whole device consists of two 316L stainless steel chambers whose volumes are 128.47 cm^3 (V_1) and 49.67 cm^3 (V_2), respectively. The bigger chamber, named as gas reservoir, isolates gases before it contacts with the IL samples in the smaller chamber. The smaller chamber used as equilibrium cell is equipped with a magnetic stirrer. The temperatures (T) of both chambers are controlled by a water bath with an uncertainty of ±0.1 K. The pressures in the two chambers are monitored using two pressure transducers of ±0.2% uncertainty. The pressure transducers are connected to a numeric instrument to record the pressure changes

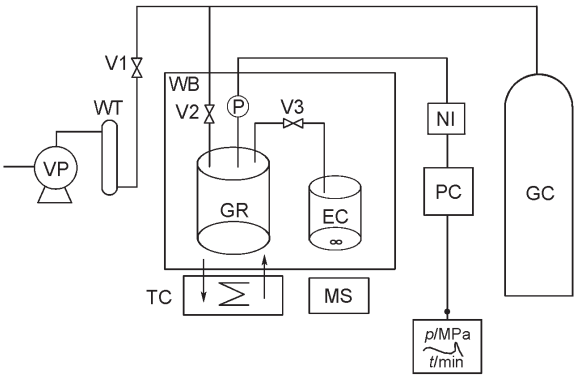

Fig.1 Device of CO_2 absorption

V: valve, P: pressure meter, VP: vacuum pump, WT: water trap, GC: gas container, GR: gas reservoir, EC: equilibrium cell, MS: magnetic stirrer, PC: personal computer, NI: numerical indicator, TC: temperature controller

online. In a typical run, about 1 mmol of IL sample was placed into the equilibrium cell and the air in the two chambers was evacuated (< 100 Pa). The pressure in the equilibrium cell was recorded to be p_0. CO_2 from its gas cylinder was fed into the gas reservior to a pressure of p_1. The needle valve between the two chambers was turned on to let gases be introduced to the equilibrium cell. Absorption equilibrium was thought to be reached when the pressures of the two chambers remained constant for at least 30 min. The equilibrium pressures were denoted as p'_1 for the gas reservior and p_2 for the equilibrium cell. The gas partial pressure in the equilibrium cell was $p_g = p_2 - p_0$. The gas uptake, $n(p_g)$, can thus be calculated using the following equation:

$$n(p_g) = \rho_g(p_1, T)V_1 - \rho_g(p'_1, T)V_1 - \rho_g(p_g, T)(V_2 - w/\rho_{IL}) \quad (1)$$

where $\rho_g(p_i, T)$ represents the density of gas in mol·cm^{-3} at p_i (i = 1, g) and T. ρ_{IL} is the density of the IL in g·cm^{-3} at T. w is the mass of IL sample. V_1 and V_2 represent the volumes in cm^3 of the two chambers, respectively. Duplicate experiments were run for each IL system to obtain averaged values of gas absorption. The averaged uncertainty of the absorption data in this work was well within ±1%.

3 Results and discussion

3.1 Density

The experimental densities of four [P_{4444}][CA] ILs are presented in Table S1 (Supporting Information), and the density dependence on temperature is plotted in Fig.2. It can be observed that the densities of these CAILs decrease linearly with the increase of temperature, and the density order is as follows: [P_{4444}][Prop] < [P_{4444}][Buty] < [P_{4444}][For] ≈ [P_{4444}][Ace]. These results show that an increase in the anion alkyl chain length directly reduces the density values for the present CAILs. This is because as the alkyl chain length of anion prolongs, the volume of CAILs would improve and thus the value of density deceases accordingly. A similar phenomenon for other CAILs reported by Muhammad and co-workers[15]. However, [P_{4444}][Buty] did not perform the smallest density, which originates from its biggest molecular weight.

3.2 Viscosity

The experimental data of the viscosities are given in Table S2 in Supporting Information, and Fig.3 shows the effect of temperature on viscosities of CAILs. It is demonstrated that the high

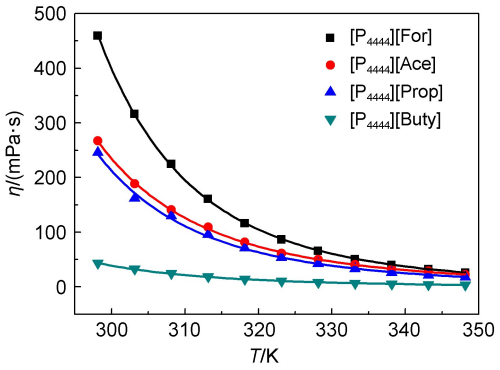

Fig.3 Viscositiy η as a function of temperature

temperature could decrease the viscosities of [P_{4444}][CA] ILs significantly. The viscosity order is as follows: [P_{4444}][Buty] < [P_{4444}][Prop] < [P_{4444}][Ace] < [P_{4444}][For]. This shows that an increase in the alkyl chain length of anions tends to reduce the viscosity of [P_{4444}][CA] ILs. When the volume of anion in CAILs increases, the interaction between anion and cation would be weakened, resulting in a relatively low value of viscosity.

3.3 Refractive Index

The measured data of the refractive indices are presented in Table S3 (Supporting Information), and the effect of temperature on refractive index is shown in Fig.4. It is found that the refractive index is linearly decreasing with the increase of temperature, and the order is [P_{4444}][Buty] < [P_{4444}][Prop] < [P_{4444}][Ace] < [P_{4444}][For], implying that a large anion can lead to a relatively low refractive index. This is explained that according to the Lorentz-Lorenz equation, the volume of its cation and anion is negative to the refractive index of [P_{4444}][CA] ILs[26]. When the size of anions grows, the value of volume becomes smaller and thus the refractive index decreases.

3.4 Conductivity

The experimental data of conductivity are listed in Table S4 (Supporting Information), and the effect of temperature on the conductivity is shown in Fig.5. It is found that the conductivity increases with increasing the temperature. Also, it has been pointed out that lower viscosity always leads to higher ionic mobility of the ILs[27]. Thus, the order of the electrical conductivities of [P_{4444}][CA] ILs is in the opposite sequence of their vis-

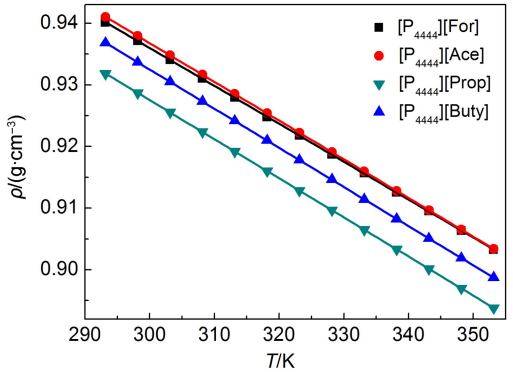

Fig.2 Densitiy ρ as a function of temperature

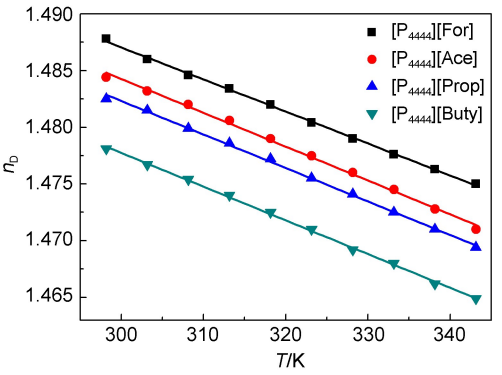

Fig.4 Refractive index n_D as a function of temperature

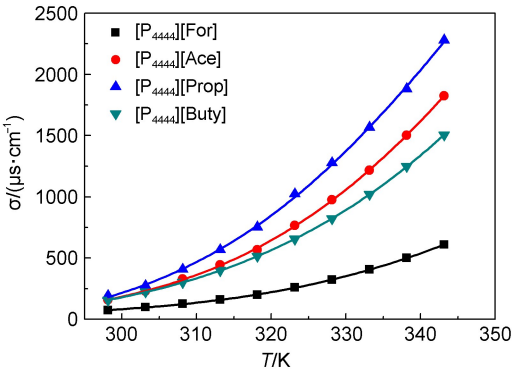

Fig.5 Conductivity σ as a function of temperature

cosities as follows: [P_{4444}][For] < [P_{4444}][Ace] < [P_{4444}][Prop]. However, it is seen that [P_{4444}][Buty] has a relatively small conductivity, even though its viscosity is the lowest among these four [P_{4444}][CA] ILs. This can be explained that the anion $[Buty]^-$ owing too high volume is hard to move and thus obtains lower ionic mobility, contributing to a relatively low electrical conductivity of the ILs.

3.5 Empirical correlation

On the basis of the above observations, the physicochemical properties were fitted to the following empirical equations as a function of temperature[24,28−30].

$$\rho = A_1 + A_2 T \tag{2}$$

$$\eta = A_3 \cdot \exp\left(\frac{A_4}{T - A_5}\right) \tag{3}$$

$$n_D = A_6 + A_7 T \tag{4}$$

$$\sigma = A_8 \cdot \exp\left(\frac{A_9}{T - A_{10}}\right) \tag{5}$$

where ρ (g·cm^{-3}), η, n_D, and σ denote are the density, viscosity, refractive index, and conductivity, respectively. A_1, A_2, A_3, A_4, A_5, A_6, A_7, A_8, A_9, and A_{10} are correlation coefficients. T is the Kelvin temperature. The correlation coefficients were estimated using linear regression analysis, and the values were reported together with the standard deviations (SD) in Tables 1−4. The SD values were calculated by using the following expression:

$$SD = \sqrt{\frac{\sum_i^N (Z_{exp} - Z_{cal})^2}{N}} \tag{6}$$

where N is the number of experimental points, Z_{exp} and Z_{cal} are the experimental and calculated values (using Eqs.(1-4)), respectively. As seen from Tables 1−4, it was noted that all the correlation coefficients were over 0.99. The temperature dependence of viscosity and conductivity could be well described by the Arrhenius and Vogel-Tamman-Fulcher (VTF) equations.

Table 1 Fitting parameter values of Eq.(1) and the standard deviations

Ionic liquid	A_1/(g·cm^{-3})	A_2/(g·cm^{-3}·K^{-1})	SD	R^2
[P_{4444}][For]	1.12047	-6.14945×10^{-4}	3.02132×10^{-8}	0.99998
[P_{4444}][Ace]	1.12512	-6.27846×10^{-4}	3.38462×10^{-9}	0.99999
[P_{4444}][Prop]	1.11784	-6.34385×10^{-4}	5.89615×10^{-9}	0.99999
[P_{4444}][Buty]	1.12307	-6.35286×10^{-4}	6.24780×10^{-9}	0.99999

R^2: correlation coefficient

Table 2 Fitting parameter values of Eq.(2) and the standard deviations

Ionic liquid	A_3/(mPa·s)	A_4/K	A_5/K	SD	R^2
[P_{4444}][For]	0.01252	1403.7159	164.640	2.58981	0.99987
[P_{4444}][Ace]	0.05047	1066.469	173.711	3.12833	0.99948
[P_{4444}][Prop]	0.02316	1192.915	169.274	17.5372	0.99660
[P_{4444}][Buty]	4.0893×10^{-4}	2128.250	114.366	0.17047	0.99899

Table 3 Fitting parameter values of Eq.(3) and the standard deviations

Ionic liquid	A_6	A_7/K^{-1}	SD	R^2
[P_{4444}][For]	1.57173	9.93428×10^{-4}	1.58061×10^{-7}	0.99892
[P_{4444}][Ace]	1.57379	0.00180	5.19879×10^{-7}	0.99682
[P_{4444}][Prop]	1.5709	0.00131	2.74909×10^{-7}	0.99828
[P_{4444}][Buty]	1.5669	0.00114	2.08970×10^{-7}	0.99871

Table 4 Fitting parameter values of Eq.(4) and the standard deviations

Ionic liquid	A_8/(μS·cm^{-1})	A_9/K	A_{10}/K	SD	R^2
[P_{4444}][For]	1.7047×10^8	−3900.5	32.068	8.35828	0.99974
[P_{4444}][Ace]	1.5759×10^5	−541.91	221.62	68.3395	0.99969
[P_{4444}][Prop]	9.7508×10^4	−421.58	231.07	506.801	0.99840
[P_{4444}][Buty]	8.0174×10^5	−1074.2	172.02	4.7094	0.99998

In addition, since the temperature−density relationship for these [P_{4444}][CA] ILs was linear, density values as a function of temperature were used to calculate the thermal expansion coefficient (α_p) (Table 5). The thermal expansion coefficients (α_p), also known as volume expansivity, as a function of temperature at atmospheric pressure were determined by using the following Eq.(7):

$$\alpha = -\frac{1}{\rho}\left(\frac{\partial \rho}{\partial T}\right)_p = -\frac{A_2}{A_1 + A_2 T} \tag{7}$$

where α_p, ρ, and T are the thermal expansion coefficient, density, and absolute temperature, respectively, whereas A_1 and A_2 are the fitting parameters of Eq.(2). As seen from Table 5, it is observed that the values of thermal expansion coefficient do not appreciably

Table 5 Thermal expansion coefficient values of [P_{4444}][CA] ILs

T/K	$10^4\alpha_p$/K^{-1}			
	[P_{4444}][For]	[P_{4444}][Ace]	[P_{4444}][Prop]	[P_{4444}][Buty]
293.15	6.54	6.67	6.81	6.78
298.15	6.56	6.69	6.83	6.80
303.15	6.58	6.72	6.85	6.83
308.15	6.61	6.74	6.88	6.85
313.15	6.63	6.76	6.90	6.87
318.15	6.65	6.78	6.93	6.90
323.15	6.67	6.81	6.95	6.92
328.15	6.69	6.83	6.97	6.95
333.15	6.72	6.85	7.00	6.97
338.15	6.74	6.88	7.02	6.99
343.15	6.76	6.90	7.05	7.02
348.15	6.78	6.93	7.07	7.04
353.15	6.81	6.95	7.10	7.07

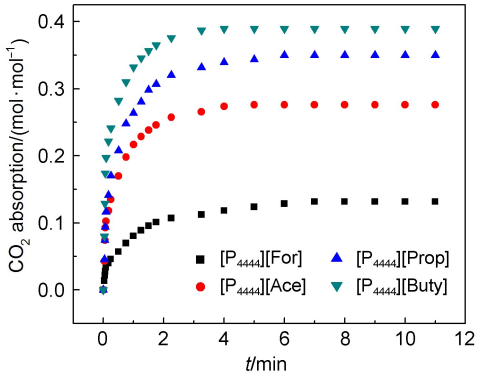

Fig.6 CO_2 absorption curves for four [P_{4444}][CA] ILs

change with temperature for the range from 298.15 to 353.15 K. The value of averaged relative deviation in α_p is found to be less than 3%. This demonstrates that the thermal expansion coefficient of [P_{4444}][CA] ILs is almost independent of temperature, and this phenomenon is also observed similar to those reported for imidazolium, pyridinium, phosphonium, and ammonium-based ILs[31,32].

3.6 CO_2 absorption

The solubilities of CO_2 in these four [P_{4444}][CA] ILs were measured at a temperature of 313.15 K and elevated pressures up to 100 kPa. The solubility data are graphically shown in Fig.6. It is significantly noted that the absorption equilibrium could all be reached within 5 min, much shorter than the time used in most of ILs [33−35]. This is primarily due to the effect of viscosity on the mass transfer of CO_2. As seen from Fig.4 and Table S2, all the viscosities of these four [P_{4444}][CA] ILs are lower than 165 mPa·s at 313.15 K, and thus low viscosity accelerates the absorption rate. Moreover, it is indicated that the anion of CAILs has an obvious effect on the CO_2 absorption capacity. Compared with other three CAILs, [P_{4444}][Buty] can absorb CO_2 with the highest solubility of 0.4 in molar fraction at 313.15 K and 100 kPa. It is known that with the prolonging carbon chain length, the basicity of carboxylic anion gradually increases because of the electrondonation of alkyl group. Thus [P_{4444}][Buty] possessing strong basicity can induce a relatively high CO_2 absorption capacity. This phenomenon is also observed similar to those reported for imidazolate-based ionic liquids[36].

4 Conclusions

The physicochemical properties of four tetrabutylphosphonium carboxylate ILs including density, viscosity, refractive index, conductivity were determined at atmospheric pressure, and CO_2 absorption capacities of these CAILs were further measured at 313.15 K. It demonstrates that the properties of there carboxylate ILs show simple systematic variations with temperature and with the alkyl chain length of the carboxylate anion. The empirical equations can be used for fitting the experimental data very well. Compared with other CAILs, [P_{4444}][Buty] has the highest capacity of 0.4 mol IL for 1 mol CO_2. This study will be significant for [P_{4444}][CA] ILs′ industrial and engineering applications.

Supporting Information: The experimental values of density, viscosity, conductivity, and refractive index have been found in this text. This information is available free of charge *via* the internet at http://www.whxb.pku.edu.cn.

References

(1) Welton, T. *Chem. Rev.* **1999,** *99*, 2071. doi: 10.1021/cr980032t

(2) Wasserscheid, P.; Keim, W. Angew. *Chem. Int. Edit.* **2000,** *39*, 3772. doi: 10.1002/1521-3773(20001103)39:21<3772::AID-ANIE3772>3.0.CO;2-5

(3) Dupont, J.; de Souza, R. F.; Suarez, P. A. Z. *Chem. Rev.* **2002,** *102*, 3667. doi: 10.1021/cr010338r

(4) Zhang, X. P.; Zhang, X. C.; Dong, H. F.; Zhao, Z. J.; Zhang, S. J.; Huang, Y. *Energy Environ. Sci.* **2012,** *5*, 6668. doi: 10.1039/c2ee21152a

(5) García, S.; Larriba, M.; García, J.; Torrecilla, J. S.; Rodríguez, F. *J. Chem. Eng. Data.* **2010,** *56*, 113. doi: 10.1021/je100982h

(6) Wang, J.; Sun, G.; Yu, L.; Wu, F.; Guo, X. *Bioresour. Technol.* **2013,** *128*, 156. doi: 10.1016/j.biortech.2012.10.098

(7) Mäki-Arvelaa, P.; Anugwom, I.; Virtanen, P.; Sjöholm, R.; Mikkola, J. P. *Industrial Crops and Products* **2010,** *32* (3), 175. doi: 10.1016/j.indcrop.2010.04.005

(8) Yue, C. B.; Mao, A. Q.; Wei, Y. Y.; Lu, M. J. *Catal. Commun.* **2008,** *9*, 1571. doi: 10.1016/j.catcom.2008.01.002

(9) Ying, A. G.; Liu, L.; Wu, G. F.; Chen, G.; Chen, X. Z.; Ye, W. D. *Tetrahedron Lett.* **2009,** *50*, 1653. doi: 10.1016/j.tetlet.2009.01.123

(10) Jiang, T.; Gao, H. X.; Han, B. X.; Zhao, G. Y.; Chang, Y. H.; Wu, W. Z.; Gao, L.; Yang, G. Y. *Tetrahedron Lett.* **2004,** *45*, 2699. doi: 10.1016/j.tetlet.2004.01.129

(11) Zhao, H.; Gary, A. B.; Song, Z. Y.; Olarongbe, O.; Tanisha, C.; Darkeysha, P. *Green Chemistry* **2008,** *10* (6), 696. doi: 10.1039/b801489b

(12) Liang, S. G.; Liu, H. Z.; Zhou, Y. X.; Jiang, T.; Han, B. X. *New J. Chem*. **2010,** *34*, 2534. doi: 10.1039/c0nj00502a

(13) Cao, Y.; Wu, J.; Zhang, J.; Li, H. Q.; Zhang, Y.; He, J. S. *Chem. Eng. J*. **2009,** *147*, 13. doi: 10.1016/j.cej.2008.11.011

(14) Tao, D. J.; Ouyang, F.; Li, Z. M.; Hu, N.; Yang, Z.; Chen, X. S. *Industrial & Engineering Chemistry Research* **2013,** *52* (48), 17111. doi: 17111. 10.1021/ie402250e

(15) Muhammad, N.; Hossain, M. I.; Man, Z.; El-Harbawi, M.; Bustam, M. A.; Noaman, Y. A.; Alitheen, N. B. M.; Hefter, G.; Yin, C. Y. *J. Chem. Eng. Data* **2012,** *57*, 2191. doi: 10.1021/je300086w

(16) Talavera-Prietoa, N. M. C.; Ferreiraa, A. G. M.; Simões, P. N.; Carvalho, P. J.; Mattedi, S.; Coutinho, J. A. P. *J. Chem. Thermodyn.* **2014,** *68*, 221. doi: 10.1016/j.jct.2013.09.010

(17) Xu, A.; Zhang, Y.; Li, Z.; Wang, J. *J. Chem. Eng. Data* **2012,** *57* (11), 3102. doi: 10.1021/je300507h

(18) Xu, A.; Wang, J.; Zhang, Y. J.; Chen, Q. T. *Industrial & Engineering Chemistry Research* **2012,** *51* (8), 3458. doi:

10.1021/ie201345t

(19) Li, C.; Yang, H. X.; Liu, R. J.; Yang, Q.; Tong, J.; Yang, J. Z. *Acta Phys. -Chim. Sin.* **2015,** *31* (1), 11. [李　驰, 杨宏旭, 刘入境, 杨　奇, 佟　静, 杨家振. 物理化学学报, **2015,** *31* (1), 11.] doi: 10.3866/PKU.WHXB201411063

(20) Li, C. P.; Li, Z.; Zou, B. X.; Liu, Q. S.; Liu, X. X. *Acta Phys. -Chim. Sin.* **2013,** *29* (10), 2157. [李长平, 李　琢, 邹本雪, 刘青山, 刘晓霞. 物理化学学报, **2013,** *29* (10), 2157.] doi: 10.3866/PKU.WHXB201307293

(21) Guan, W.; Ma, X. X.; Li, L.; Tong, J.; Fang, D. W; Yang, J. Z. *J. Phys. Chem. B* **2011,** *115*, 12915. doi: 10.1021/jp207882t

(22) Tong, J.; Ma, X.; Kong, Y. X.; Chen, Y.; Guan, W.; Yang, J. Z. *J. Phys. Chem. B* **2012,** *116*, 5971. doi: 10.1021/jp301985g

(23) Ma, X. X.; Wei, J.; Zhang, Q. B.; Tian, F.; Feng, Y. Y.; Guan, W. *Industrial & Engineering Chemistry Research* **2013,** *52*, 9490. doi: 10.1021/ie401130d

(24) Muhammad, N.; Man, Z. B.; Bustam, M. A.; Mutalib, M. I. A.; Wilfred, C. D.; Rafiq, S. *J. Chem. Eng. Data* **2011,** *56*, 3157. doi: 10.1021/je2002368

(25) Zhang, X. M.; Huang, K.; Xia, S.; Chen, Y. L.; Wu, Y. T.; Hu, X. B. *Chem. Eur. J*. **2009,** *274*, 30. doi: 10.1016/j.cej.2015.03.052

(26) Wang, Z. X.; Chen, J. S.; Gu, M. X.; He, G. T.; Dai, P. F.; Li, M. *Journal of Functional Materials* **2012,** *16* (43), 2251. [王仲勋, 陈吉胜, 谷明信, 何国田, 戴鹏飞, 李　明. 功能材料, **2012,** *16* (43), 2251.] doi: 10.3969/j.issn.1001-9731.2012.16.032

(27) Liu, Q. S.; Yan, P. F.; Yang, M.; Tan, Z. C.; Li, C. P.; Welz-Biermann, U. *Acta Phys. -Chim. Sin*. **2011,** *27* (12), 2762. [刘青山, 颜佩芳, 杨　淼, 谭志诚, 李长平, Welz-Biermann, U. 物理化学学报, **2011,** *27* (12), 2762.] doi: 10.3866/PKU.WHXB20112762

(28) Machanová, K.; Boisset, A.; Sedláková, Z.; Anouti, M.; Bendová, M.; Jacquemin, J. *J. Chem. Eng. Data* **2012,** *57*, 2227. doi: 10.1021/je300108z

(29) Ziyada, A. K.; Bustam, M. A.; Wilfred, C. D.; Murugesan, T. *J. Chem. Eng. Data* **2011,** *56*, 2343. doi: 10.1021/je101316g

(30) Yunus, N. M.; Mutalib, M. I. A.; Man, Z.; Bustam, M. A.; Murugesan, T. *J. Chem. Thermodyn.* **2010,** *42*, 491. doi: 10.1016/j.jct.2009.11.004

(31) Gu, Z.; Brennecke, J. F. *J. Chem. Eng. Data* **2002,** *47*, 339. doi: 10.1021/je010242u

(32) Tariq, M.; Forte, A. S.; Gomes, F. C.; Lopes, N. C.; Rebelo, P. N. *J. Chem. Thermodyn.* **2009,** *41*, 790. doi: 10.1016/j.jct.2009.01.012

(33) Wang, C. M.; Luo, H. M.; Li, H. R.; Zhu, X.; Yu, B.; Dai, S. *Chem. Eur. J*. **2012,** *18*, 2153 . doi: 10.1002/chem.201103092

(34) Wang, C. M.; Luo, H. M.; Luo, X. Y.; Li, H. R.; Dai, S. *Green Chem*. **2010,** *12*, 2019. doi: 10.1039/c0gc00070a

(35) Jiang, Y. Y.; Wang, G. N.; Zhou. Z.; Wu, Y. T.; Geng. J.; Zhang, Z. B. *Chemical Communications* **2008,** *4*, 505. doi: 0.1039/B713648J

(36) Zhang, Y.; Wu, Z. K.; Chen, S. L.; Yu, P.; Luo, Y. B. *Industrial & Engineering Chemistry Research* **2013,** *52* (18), 6069. doi: 10.1021/ie302928v

Supporting Information for *Acta Phys. -Chim. Sin.* 2016, *32* (3), 605-610
doi: 10.3866/PKU.WHXB201512241

四丁基季鏻羧酸盐离子液体的物理化学性质与 CO_2 溶解度

陈凤凤　　董　艳　　桑晓燕　　周　言*　　陶端健*

(江西师范大学化学化工学院，南昌 330022)

Physicochemical Properties and CO_2 Solubility of Tetrabutylphosphonium Carboxylate Ionic Liquids

CHEN Feng-Feng　　DONG Yan　　SANG Xiao-Yan　　ZHOU Yan*　　TAO Duan-Jian*

(*College of Chemistry and Chemical Engineering, Jiangxi Normal University, Nanchang 330022, P. R. China*)

*Corresponding authors. TAO Duan-Jian, Email: djtao@jxnu.edu.cn.
ZHOU Yan, Email: anitachow@jxnu.edu.cn; Tel: +86-791-88120317.

Table S1 Experimental densities for [P_{4444}][CA] ILs as a function of temperature

T/K	ρ/(g·cm^{-3})			
	[P_{4444}][For]	[P_{4444}][Ace]	[P_{4444}][Prop]	[P_{4444}][Buty]
293.15	0.94011	0.94103	0.93182	0.93678
298.15	0.93713	0.93792	0.92869	0.93366
303.15	0.93406	0.93480	0.92555	0.93051
308.15	0.93101	0.93167	0.92239	0.92734
313.15	0.92794	0.92853	0.91921	0.92416
318.15	0.92478	0.92538	0.91603	0.92097
323.15	0.92179	0.92224	0.91285	0.91779
328.15	0.91872	0.91909	0.90967	0.91461
333.15	0.91564	0.91595	0.90649	0.91142
338.15	0.91257	0.91280	0.90331	0.90824
343.15	0.90949	0.90966	0.90014	0.90507
348.15	0.90633	0.90652	0.89698	0.90189
353.15	0.90322	0.90341	0.89381	0.89872

[a]standard uncertainties *u* are $u(T)$ = 0.05 K, $u(p)$ = 10 kPa, and $u_r(\rho)$ = 3.16*10^{-5} g·cm^{-3}.

Table S2 Experimental dynamic viscosities for $[P_{4444}][CA]$ ILs as a function of temperature

T/K	η/(mPa s)			
	$[P_{4444}]$For]	$[P_{4444}]$ [Ace]	$[P_{4444}]$ [Prop]	$[P_{4444}]$ [Buty]
298.15	459.6	267.0	245.6	43.2
303.15	316.3	188.6	162.1	32.7
308.15	224.5	140.7	129.5	24.6
313.15	160.7	109.1	95.8	18.6
318.15	116.0	81.7	70.8	14.0
323.15	86.5	61.3	53.3	10.6
328.15	65.7	50.2	42.2	8.41
333.15	50.5	40.6	32.8	6.48
338.15	39.9	32.4	26.1	5.28
343.15	32.2	28.6	21.4	4.30
348.15	26.1	22.2	17.6	3.56

[a]Standard uncertainties u are $u(T) = 0.05$ K, $u(p) = 10$ kPa, and the relative standard uncertainty for viscosity $u_r(\eta) = 3.16*10^{-2}$ mPa s

Table S3 Experimental refractive indices for [P_{4444}][CA] ILs as a function of temperature

T/K	n_D			
	[P_{4444}]For]	[P_{4444}] [Ace]	[P_{4444}] [Prop]	[P_{4444}] [Buty]
298.15	1.4878	1.4844	1.4825	1.4781
303.15	1.4860	1.4832	1.4815	1.4767
308.15	1.4846	1.4820	1.4799	1.4754
313.15	1.4834	1.4806	1.4786	1.4740
318.15	1.4820	1.4790	1.4772	1.4725
323.15	1.4804	1.4775	1.4755	1.4710
328.15	1.4790	1.4760	1.4741	1.4692
333.15	1.4776	1.4745	1.4725	1.4680
338.15	1.4763	1.4728	1.4710	1.4662
343.15	1.4750	1.4710	1.4694	1.4649

[a]Standard uncertainties u are $u(T)$ = 0.05 K, $u(p)$ = 10 kPa, and $u_r(n_D)$ = 3.16*10^{-4}.

Table S4 Experimental conductivity for [P_{4444}][CA] ILs as a function of temperature

T/K	σ/(μs cm^{-1})			
	[P_{4444}]For]	[P_{4444}] [Ace]	[P_{4444}] [Prop]	[P_{4444}] [Buty]
298.15	74.1	16.03	186.4	156.5
303.15	98.2	27.8	281	224
308.15	126.2	57.0	410	302
313.15	159.6	211	573	398
318.15	198.7	567	752	515
323.15	259	768	1024	655
328.15	323	975	1277	823
333.15	405	1218	1566	1020
338.15	501	1503	1881	1249
343.15	609	1826	2280	1506

[a]Standard uncertainties u are $u(T)$ = 0.05 K, $u(p)$ = 10 kPa, and $u_r(\sigma)$ = 0.316μs cm^{-1}.